EPFL
École polytechnique fédérale de Lausanne

Institute of Materials - Institute of Bioengineering
sunmil.epfl.ch

SuNMiL
Supramolecular NanoMaterials and Interfaces Laboratory

Coherent and Semi-coherent Grain Boundaries
Lesson 10

MSE 304

Francesco Stellacci

桑缪 썬밀 सानमिल ΣουNMιΛ سنمل СаНМПЛ

Key Topics in the Previous Class

Coincidence Lattice Description of a Generic Grain Boundaries

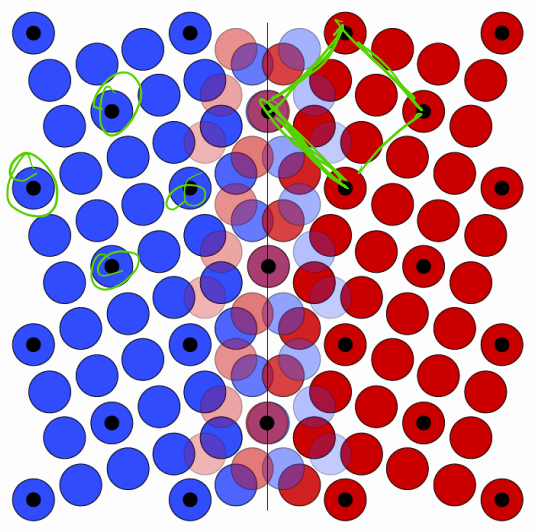

sc, $\mathbf{n} = (100)$,
$\mathbf{u} = \langle 001 \rangle$, $\theta = 36.9°$

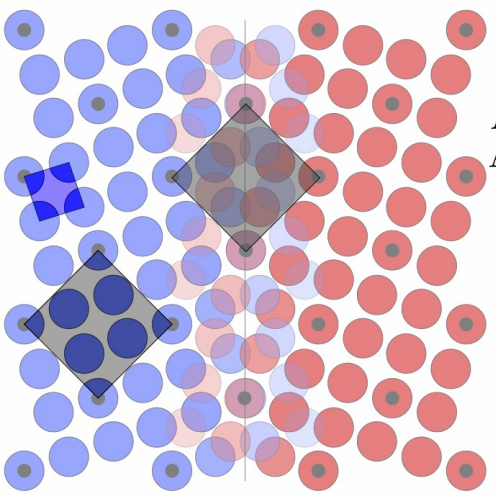

Atoms per unit cell: 1
Atoms per CSL cell: 5

$\boxed{\Sigma = 5}$

sc, $\mathbf{n} = (100)$,
$\mathbf{u} = \langle 001 \rangle$, $\theta = 36.9°$

Coincidence Lattice Description of a Generic Grain Boundaries

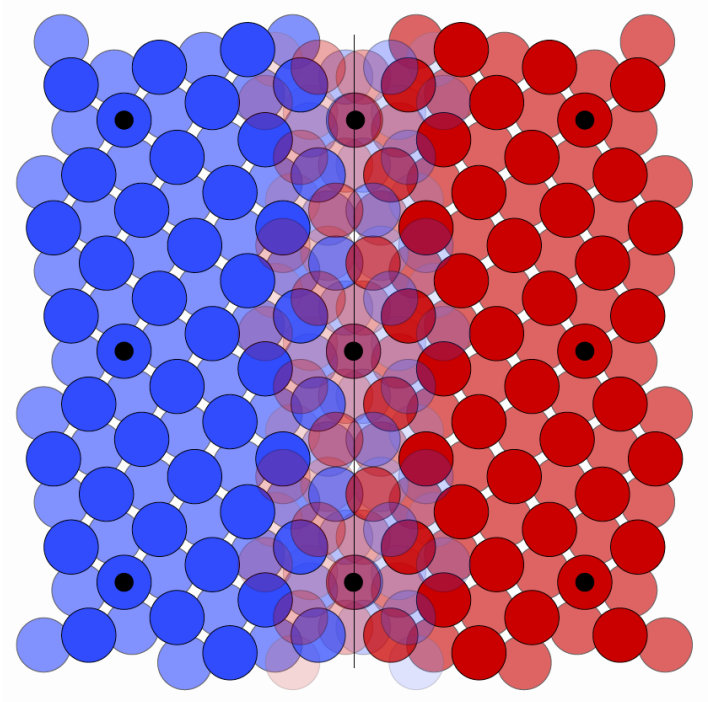

fcc, $\mathbf{n} = (100)$,
$\mathbf{u} = \langle 001 \rangle$, $\theta = 22.6°$
$\boxed{\Sigma = 13a}$

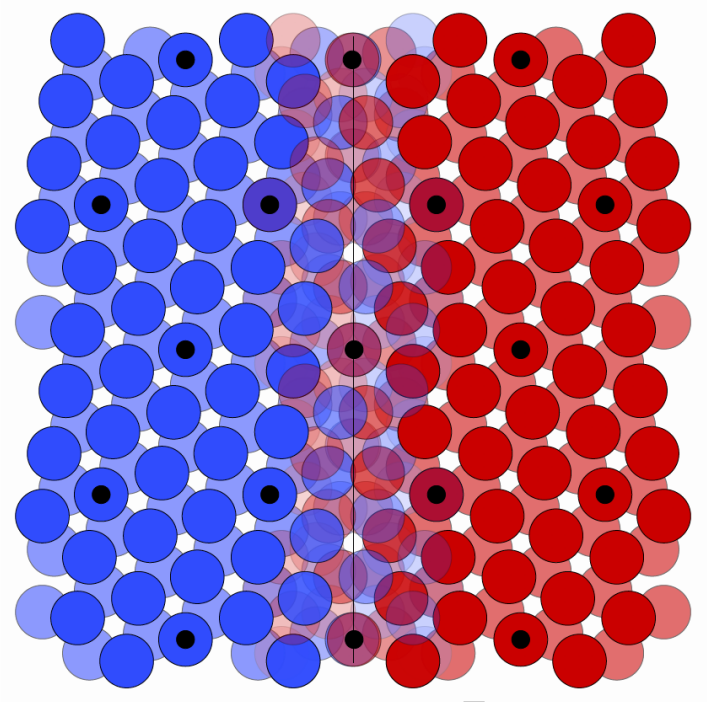

fcc, $\mathbf{n} = (1\bar{1}0)$,
$\mathbf{u} = \langle 111 \rangle$, $\theta = 38.21°$
$\boxed{\Sigma = 7}$

CSL Selection Rules

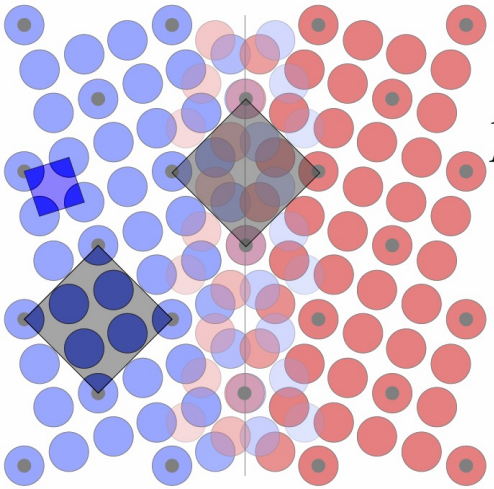

Atoms per unit cell: 1
Atoms per CSL cell: 5

$\boxed{\Sigma = 5}$

sc, $\mathbf{n} = (100)$,
$\mathbf{u} = \langle 001 \rangle$, $\theta = 36.9°$

$$\boldsymbol{\Sigma = x^2 + Ny^2}$$

$$\boldsymbol{N = u^2 + v^2 + w^2}$$

$$\boldsymbol{\theta = 2\tan^{-1}\left(\frac{y}{x}\right) N^{\frac{1}{2}}}$$

Displacement Shift Complete Lattice

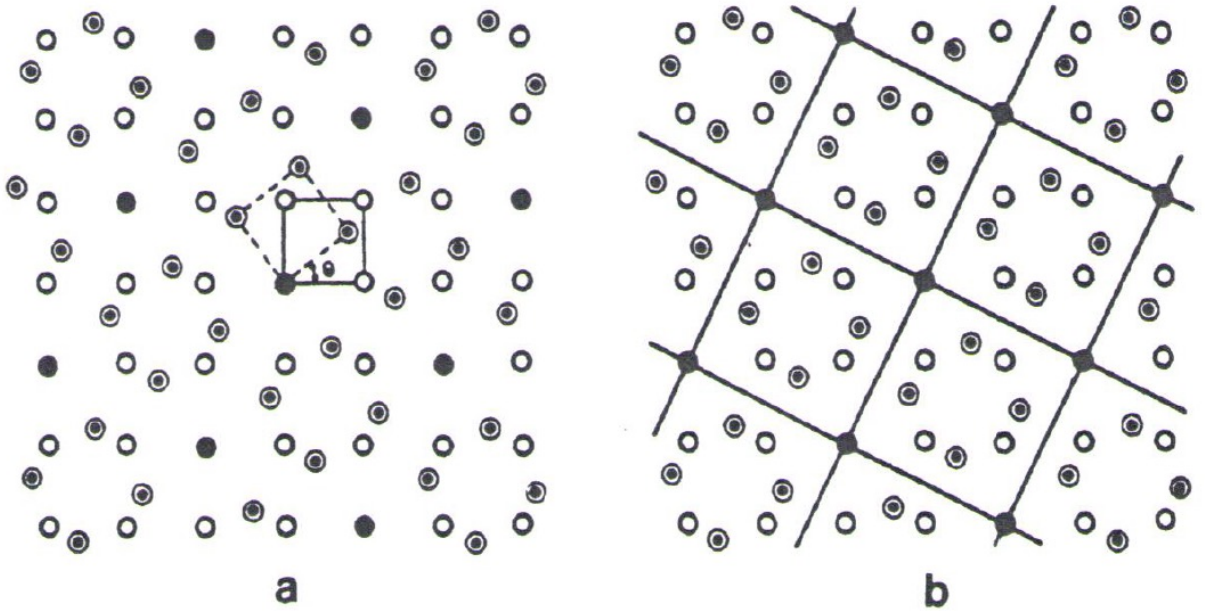

Displacement Shift Complete Lattice

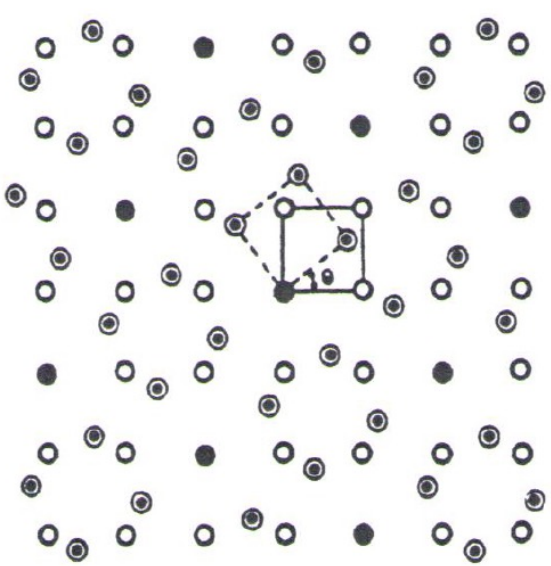

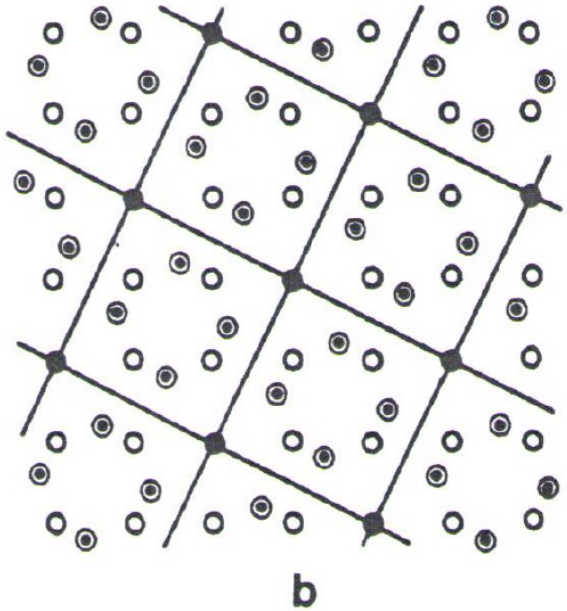

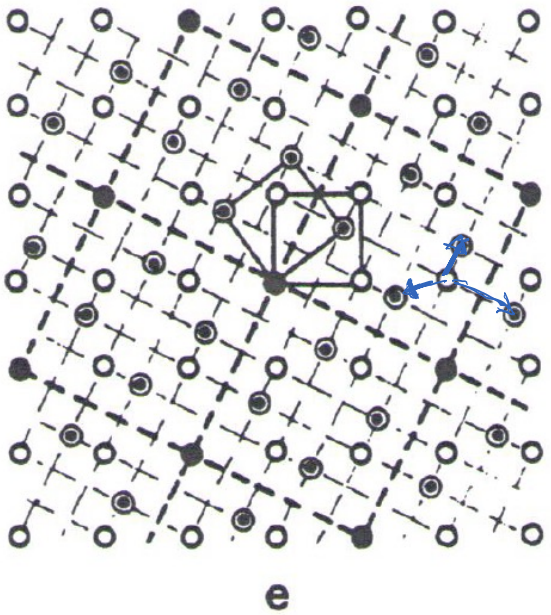

Displacement Shift Complete Lattice

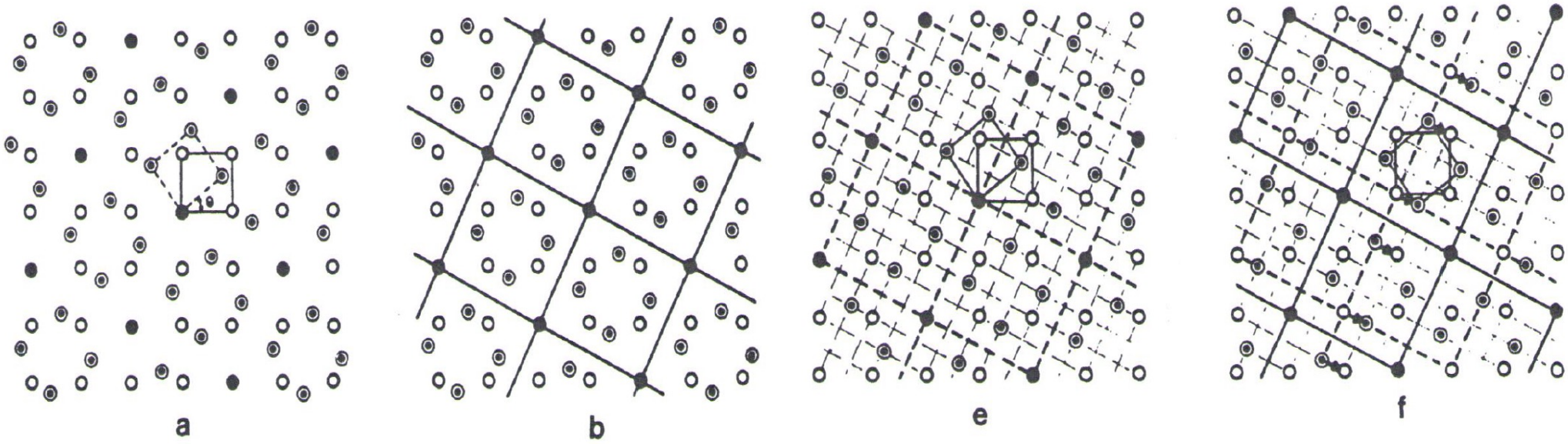

Defects at a Coherent Homophase Interfase (CHI)

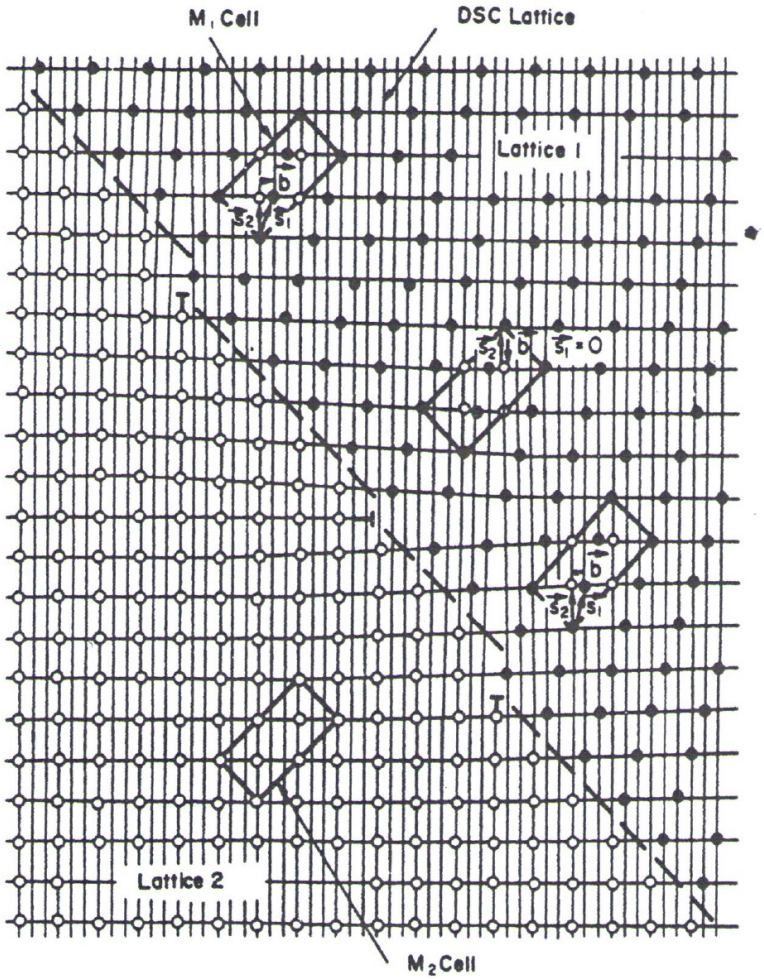

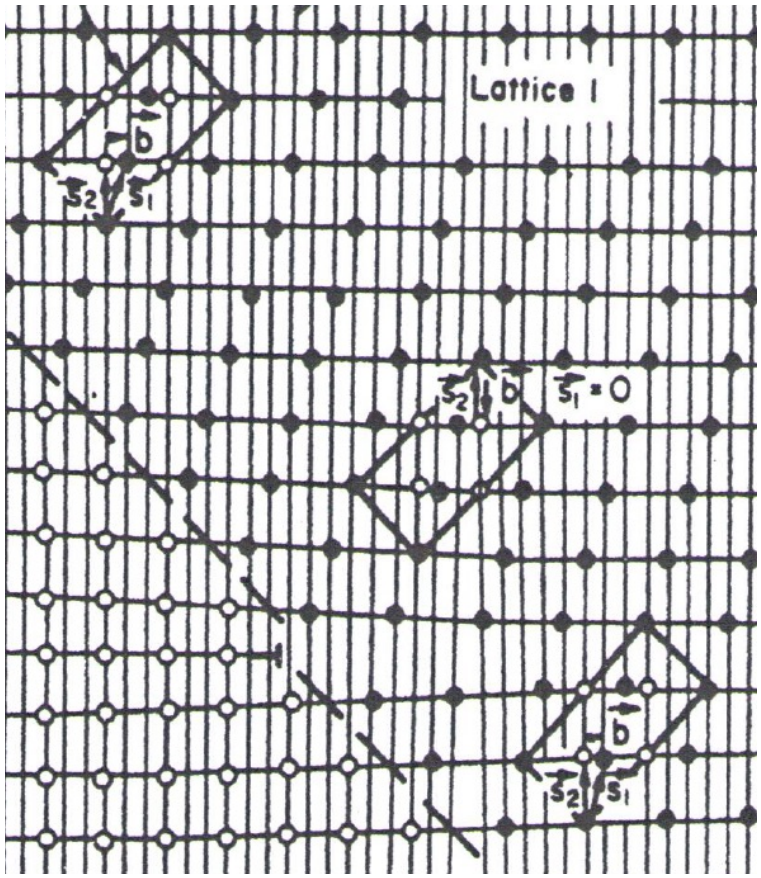

Ledges and Grain Boundaries

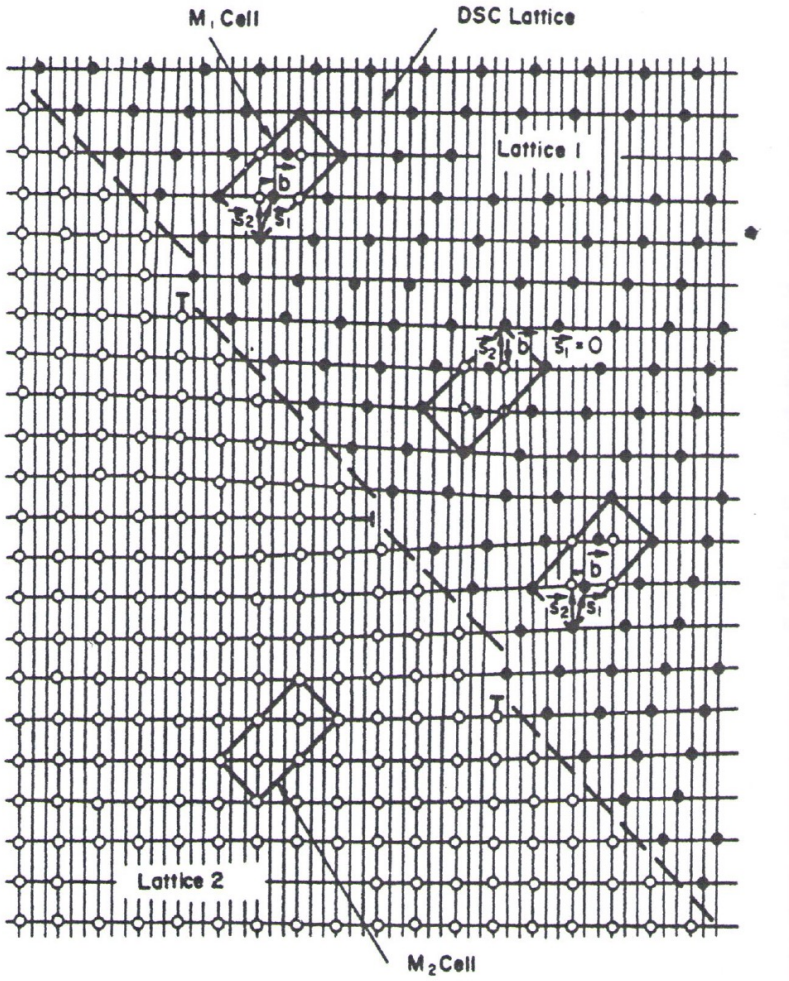

Misfit Dislocation in CHI

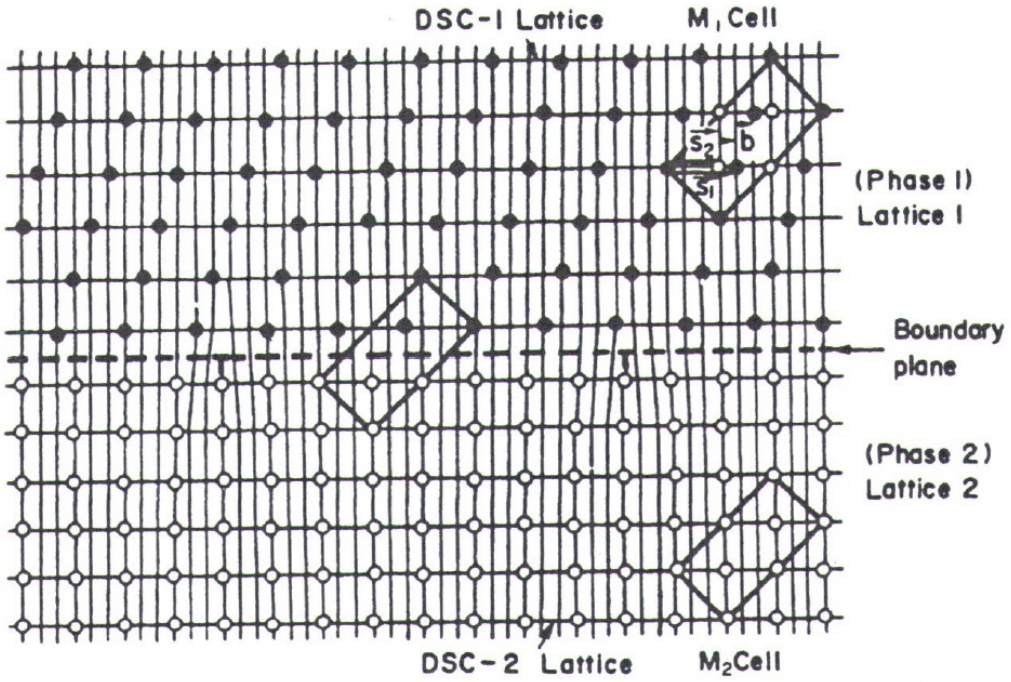

Figure 13.24. The interphase boundary between two different lattices (phases) M_1 and M_2, which form a planar interface containing interfacial dislocations with a spacing determined by O-lattice theory. The Burgers vector and ledge vectors of the interfacial dislocations are shown in the diagram in the upper right. The DSC lattice is indicated by fine lines in the figure. Reprinted with permission from [53] by Elsevier Science Ltd., Oxford, England.

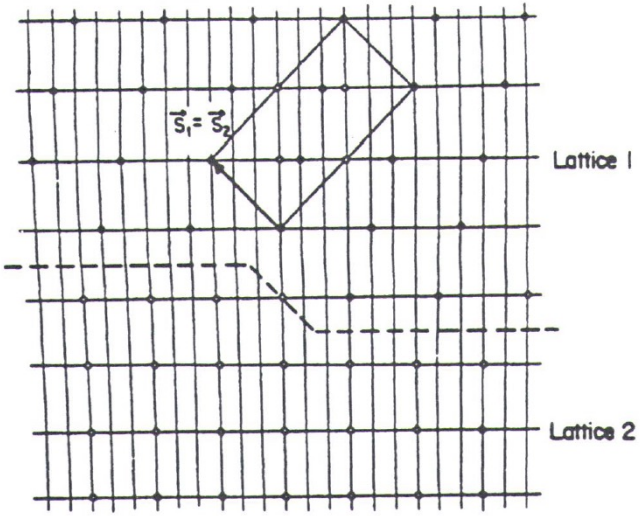

Figure 13.26. Pure ledge in the interphase boundary illustrated previously in Figure 13.24. The ledge vectors are shown above the ledge. Reprinted with permission from [53] by Elsevier Science Ltd., Oxford, England.

Misfit Dislocations in Semi-coherent Interfaces

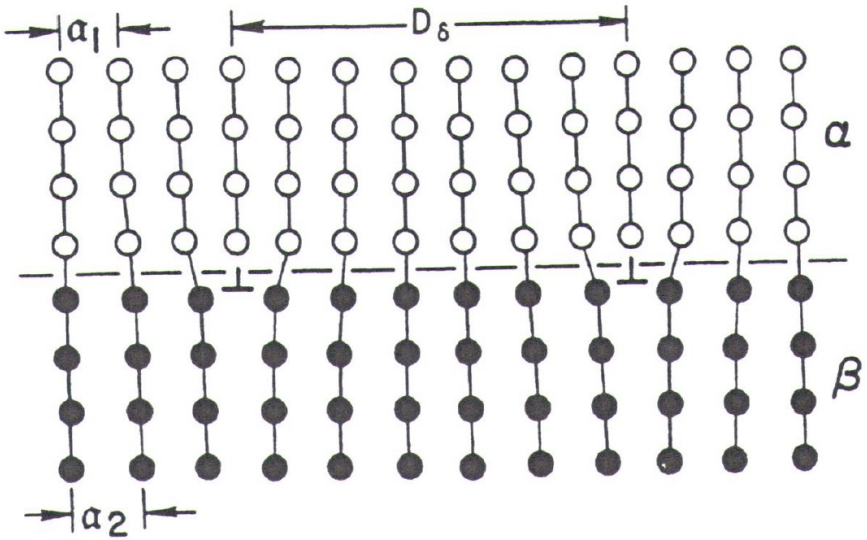

Misfit Dislocations in Semi-coherent Interfaces

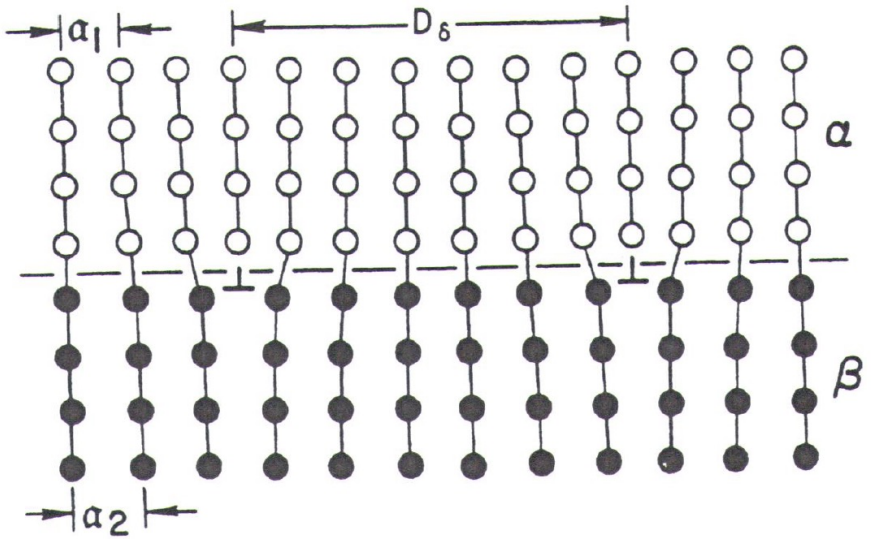

$$D_\delta = n a_1 = (n+1) a_2 \qquad n = \frac{a_2}{a_1 - a_2}$$

$$a' = \frac{a_1 + a_2}{2}$$

$$D_\delta = \left(n + \frac{1}{2}\right) a'$$

$$D_\delta = \frac{(a_1 + a_2)^2}{4(a_1 - a_2)}$$

$$\delta = \frac{2(a_1 - a_2)}{a_1 + a_2} = \frac{a_1 - a_2}{a'}$$

$$D_\delta = \frac{a'}{\delta} = \frac{b}{\delta}$$

Twin Boundaries

- Close-packed *fcc* have very low-energy **twin** grain boundaries, that correspond to reversal of the ABCABC stacking order

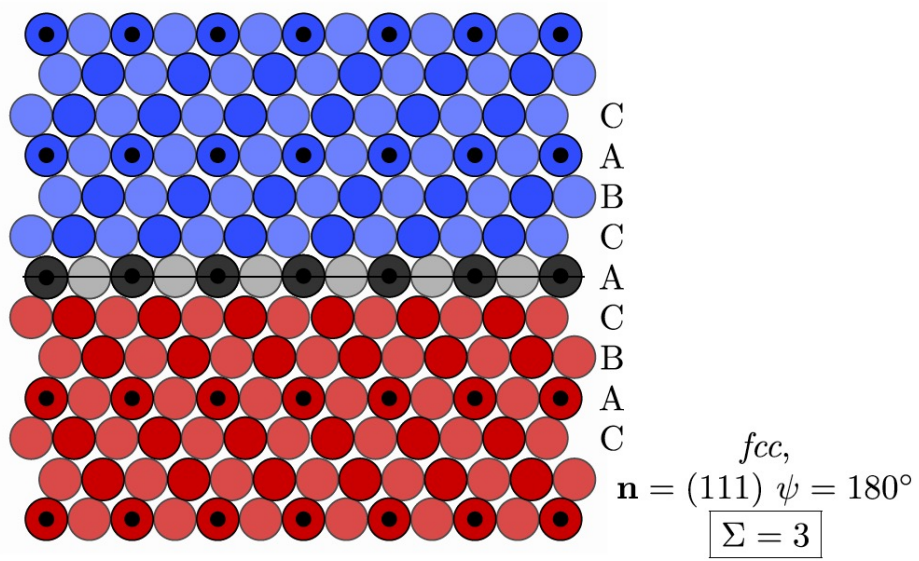

Stacking Faults

- Twins are closely related to **stacking faults**, ABCBCAB or ABCBABC

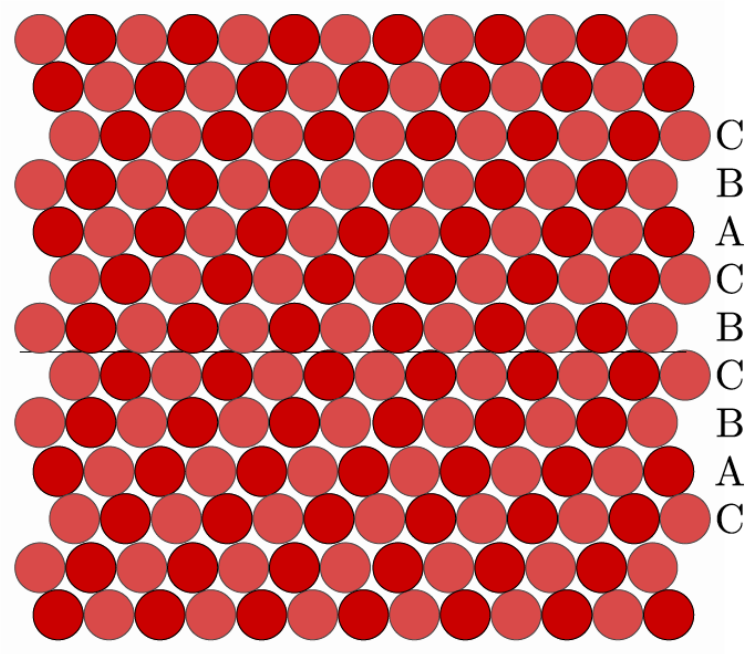

fcc,
$\mathbf{n} = (111)$

Stacking Faults and Twin Boundaries

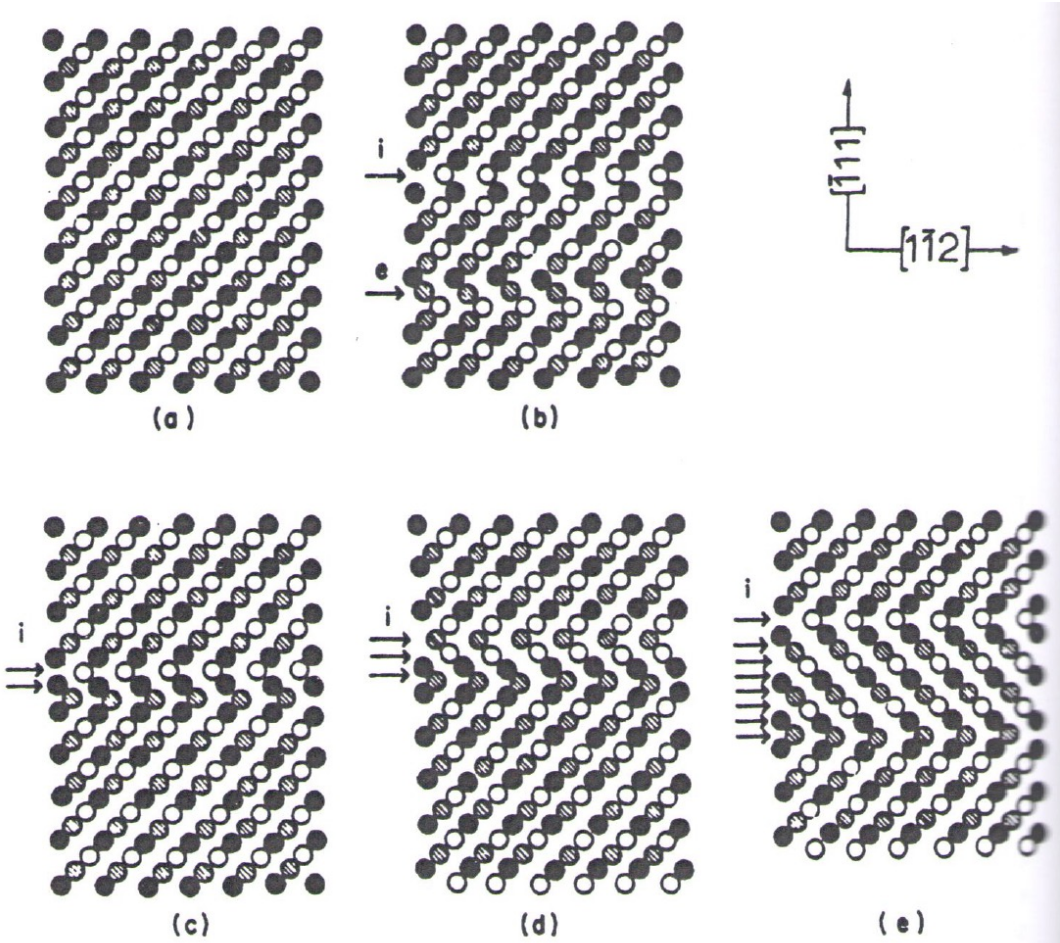

Figure 13.34. Idealized view of stacking faults and their development from perfect crystal in (a) to an *n*-layer twin in (e) in the close-packed f.c.c. structure. The viewing direction is along [110]. From [24].

Stacking Faults

- Twins are closely related to **stacking faults**, ABCBCAB or ABCBABC
  - Stacking faults can be thought as a pair of twins, and in fact $\gamma_{sf} \approx 2\gamma_t$

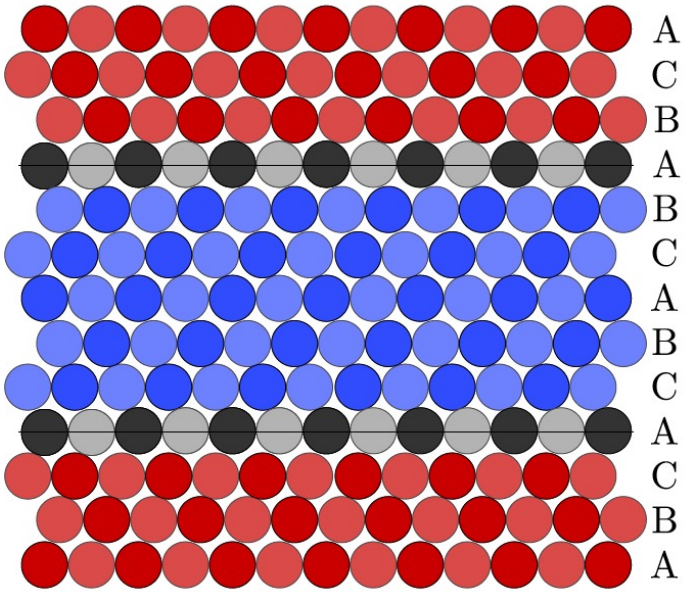

fcc,
$\mathbf{n} = (111)$

Segregation at Domain Boundaries

- The type, stability, and mechanical properties of grain boundaries can be tuned by the presence of impurities
- Interstitial or substitutional impurities can segregate at grain boundaries because they can better accommodate lattice mismatch
- Gibbs absorption equation holds: $\frac{\partial \gamma}{\partial c} \approx -\Gamma / c$. Segregating atoms lower γ_{GB}

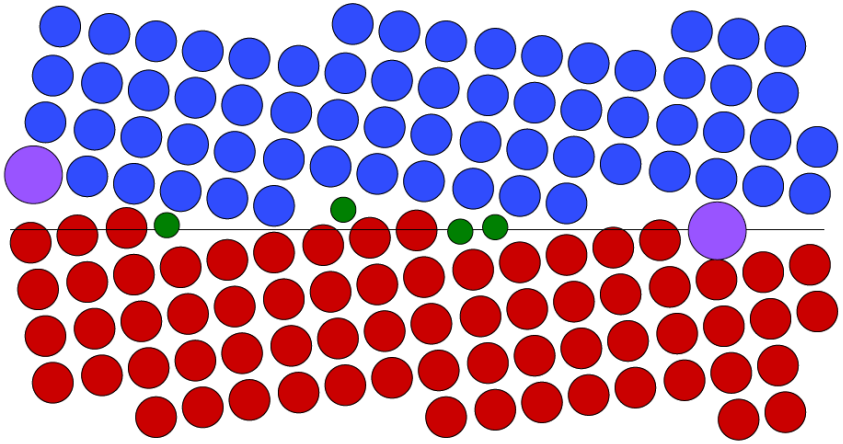

sc, $\mathbf{u} = \langle 001 \rangle$,
$\mathbf{n} = (100)$, $\theta = 18°$

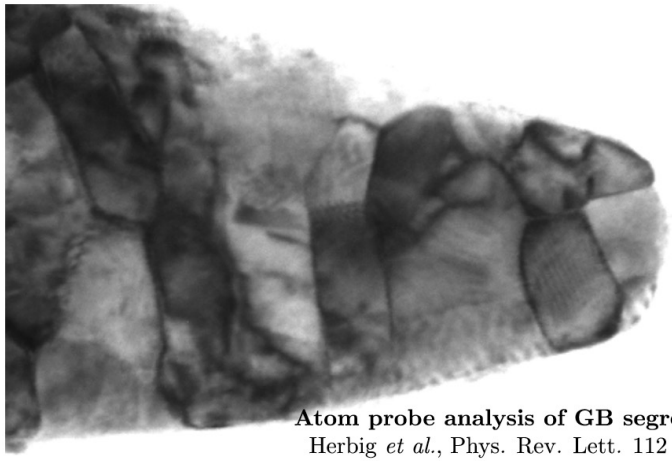

Atom probe analysis of GB segregation
Herbig *et al.*, Phys. Rev. Lett. 112 (2014)
Li *et al.*, Phys. Rev. Lett. 113 (2014)

Segregation at Domain Boundaries

- The type, stability, and mechanical properties of grain boundaries can be tuned by the presence of impurities
- Interstitial or substitutional impurities can segregate at grain boundaries because they can better accommodate lattice mismatch
- Gibbs absorption equation holds: $\frac{\partial \gamma}{\partial c} \approx -\Gamma / c$. Segregating atoms lower γ_{GB}

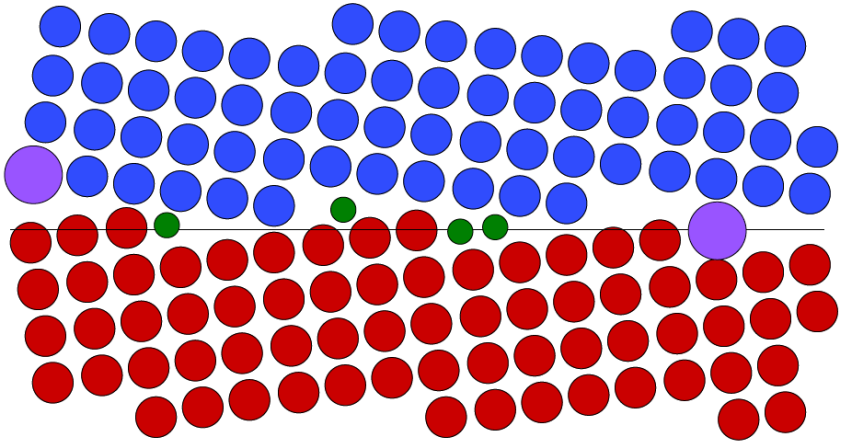

sc, $\mathbf{u} = \langle 001 \rangle$,
$\mathbf{n} = (100)$, $\theta = 18°$

$$\frac{X_{gb}}{1 - X_{gb}} = \frac{X_B}{X_B^{sat}} \exp \frac{-\Delta G'}{RT}, \qquad (13.40)$$

$$\beta_{gb} = \frac{1}{X_B^{sat}} \exp \frac{-\Delta G'}{RT}. \qquad (13.42)$$

Coherent Interfaces: The Cahn Hillard Model

Coherent Interfaces: The Cahn Hillard Model

$$f\left(c, \nabla c, \nabla^2 c, \dots\right) = f_0 + \sum_i L_i \nabla_i c + \sum_{i,j} k_{ij}^{(1)} \frac{\partial^2 c}{\partial x_i \partial x_j} + \frac{1}{2} \sum_{i,j} k_{ij}^{(2)} \frac{\partial c}{\partial x_i} \frac{\partial c}{\partial x_j} + \cdots$$

$$L_i = \frac{\partial f}{\partial \left(\partial c / \partial x_i \right)}$$

$$k_{ij}^{(1)} = \frac{\partial f}{\partial \left(\frac{\partial^2 c}{\partial x_i \partial x_j} \right)}$$

$$k_{ij}^{(2)} = \frac{\partial^2 f}{\partial \left(\partial c / \partial x_i \right) \partial \left(\partial c / \partial x_j \right)}$$

Coherent Interfaces: The Cahn Hillard Model

$$\boldsymbol{f\left(c, \nabla c, \nabla^2 c, \ldots\right) = f_0 + \sum_i L_i \nabla_i c + \sum_{i,j} k_{ij}^{(1)} \frac{\partial^2 c}{\partial x_i \partial x_j} + \frac{1}{2} \sum_{i,j} k_{ij}^{(2)} \frac{\partial c}{\partial x_i} \frac{\partial c}{\partial x_j} + \cdots}$$

$$L_i = \frac{\partial f}{\partial \left({}^{\partial c}/_{\partial x_i} \right)} \qquad L_i = 0$$

$$k_{ij}^{(1)} = \frac{\partial f}{\partial \left(\frac{\partial^2 c}{\partial x_i \partial x_j} \right)} \qquad k_{ij}^{(1)} = k^1 = \frac{\partial f}{\partial (\nabla^2 c)} \; for \; i = j \; ; \qquad k_{ij}^{(1)} = 0 \; otherwise$$

$$k_{ij}^{(2)} = \frac{\partial^2 f}{\partial \left({}^{\partial c}/_{\partial x_i} \right) \partial \left({}^{\partial c}/_{\partial x_j} \right)} \qquad k_{ij}^{(2)} = k^2 = \frac{\partial^2 f}{\partial \left(|\nabla c|^2 \right)^{1/2}} \; for \; i = j \; ; \qquad k_{ij}^{(2)} = 0 \; otherwise$$

$$\boldsymbol{f\left(c, \nabla c, \nabla^2 c, \ldots\right) = f_0 + \sum_i k^1 \frac{\partial^2 c}{\partial^2 x_i} + \sum_i k^2 \left(\frac{\partial c}{\partial x_i} \right)^2 + \cdots = f_0 + k^1 \nabla^2 c + k^2 (\nabla c)^2 + \cdots}$$

Coherent Interfaces: The Cahn Hillard Model

$$\boldsymbol{F = \int \mu dN = N_V \int_V f dV = N_V \int_V \left(f_0 + k^1 \nabla^2 c + k^2 (\nabla c)^2\right) dV}$$

Divergence Theorem:

$$\int_V k^1 \nabla^2 c dV = -\int_V \frac{dk^1}{dc} (\nabla c)^2 dV + \int_S k^1 \nabla c * n dS$$

$$\boldsymbol{F = N_V \int_V \left(f_0 + k^1 \nabla^2 c + k^2 (\nabla c)^2\right) dV = N_V \int_V \left(f_0 - \frac{dk^1}{dc} (\nabla c)^2 + k^2 (\nabla c)^2\right) dV = N_V \int_V \left(f_0 + k (\nabla c)^2\right) dV}$$

$$\boldsymbol{k = k^2 - \frac{dk^1}{dc} = \frac{\partial^2 f}{\partial (|\nabla c|^2)^{1/2}} - \frac{d}{dc}\left(\frac{\partial f}{\partial (\nabla^2 c)}\right)}$$

Coherent Interfaces: The Cahn Hillard Model

- Take x_A moles of compound A, and $x_B = 1 - x_A$ moles of compound B, and **physically** mix them
- Assume only the entropy of solution matters (**ideal solution**)

$$\mu_{A,B} = \mu^{\ominus}_{A,B} + RT \ln x_{A,B}$$

- Add an enthalpy of mixing term $\Omega x_A x_B$ (**regular solution**)

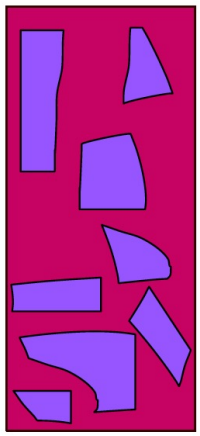

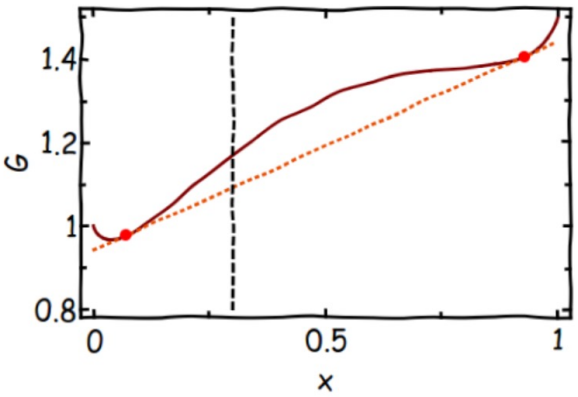

$$\mu^{\ominus}_{A} = 1 \qquad \mu^{\ominus}_{B} = 1.5$$
$$RT = 1 \qquad \Omega = 2.5$$

$$G = x_A \left(\mu^{\ominus}_{A} + RT \ln x_A\right) + (1 - x_A)\left(\mu^{\ominus}_{B} + RT \ln (1 - x_A)\right) + \Omega x_A (1 - x_A)$$

Coherent Interfaces: The Cahn Hillard Model

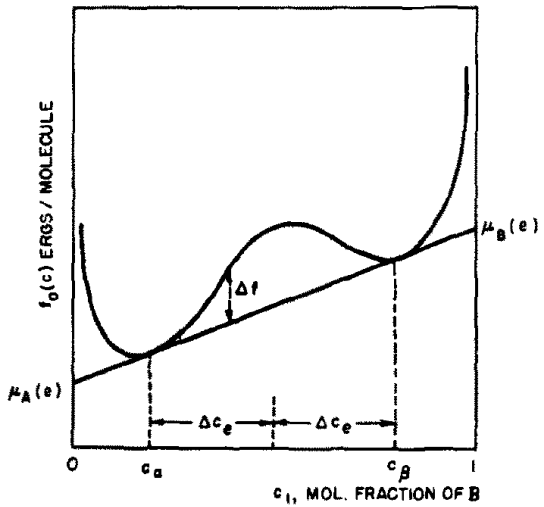

FIG. 1. $f_0(c)$ for $T<T_c$.

$$F = N_V \int_V \left(f_0 + k(\nabla c)^2\right) dV = N_V A \int_{-\infty}^{+\infty} \left(f_0 + k\left(\frac{dc}{dx}\right)^2\right) dx$$

$$\gamma = N_V \int_{-\infty}^{+\infty} \left[f_0 + k\left(\frac{dc}{dx}\right)^2 - c\mu_\beta(e) - (1-c)\mu_\alpha(e)\right] dx$$

$$\gamma = N_V \int_{-\infty}^{+\infty} \left[\Delta f(c) + k\left(\frac{dc}{dx}\right)^2\right] dx$$

Coherent Interfaces: The Cahn Hillard Model

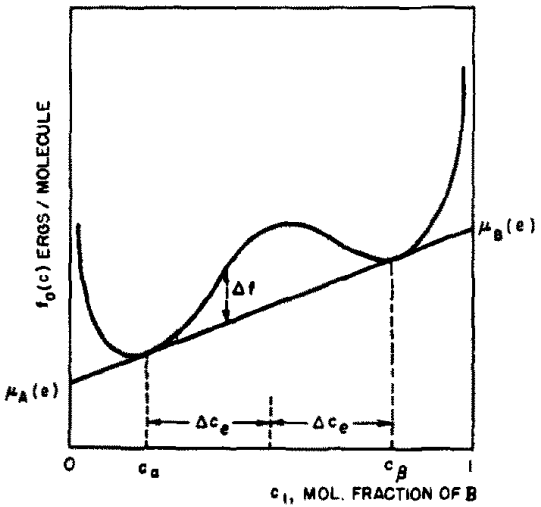

FIG. 1. $f_0(c)$ for $T<T_c$.

$$\gamma = N_V \int_{-\infty}^{+\infty} \left[\Delta f(c) + k\left(\frac{dc}{dx}\right)^2\right] dx$$

Euler equation:

$$I - \left(\frac{dc}{dx}\right)\left[\frac{\partial I}{\partial\left(\frac{dc}{dx}\right)}\right] = 0$$

$$\Delta f(c) - k\left(\frac{dc}{dx}\right)^2 = 0$$

$$\Delta f(c) = k\left(\frac{dc}{dx}\right)^2$$

$$dx = \left(\frac{k}{\Delta f(c)}\right)^{1/2} dc$$

$$\gamma = 2N_V \int_{-\infty}^{+\infty} \Delta f(c)\, dx$$

$$\gamma = 2N_V \int_{c_\alpha}^{c_\beta} \left(k\Delta f(c)\right)^{1/2} dc$$

SuNMIL EPFL

Coherent Interfaces: The Cahn Hillard Model

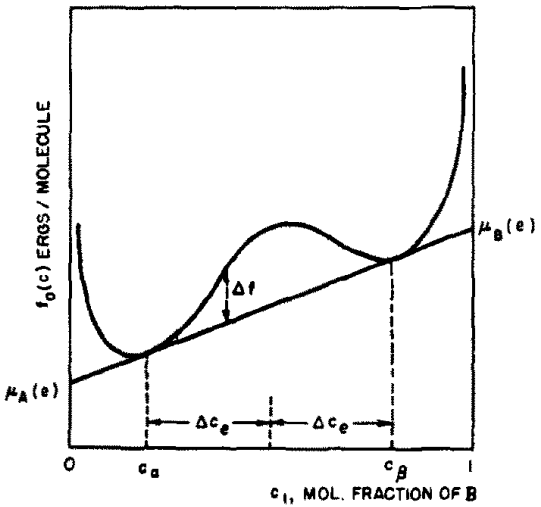

FIG. 1. $f_0(c)$ for $T<T_c$.

$$\gamma = 2N_V \int_{c_\alpha}^{c_\beta} \left(k\Delta f(c)\right)^{1/2} dc$$

$$dx = \left(\frac{k}{\Delta f(c)}\right)^{1/2} dc \qquad \frac{dc}{dx} = \left(\frac{k}{\Delta f(c)}\right)^{1/2}$$

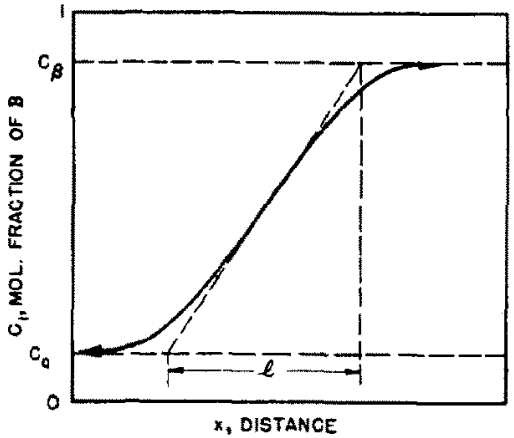

FIG. 2. Interface profile.

SuNMIL EPFL

Coherent Interfaces: The Cahn Hillard Model

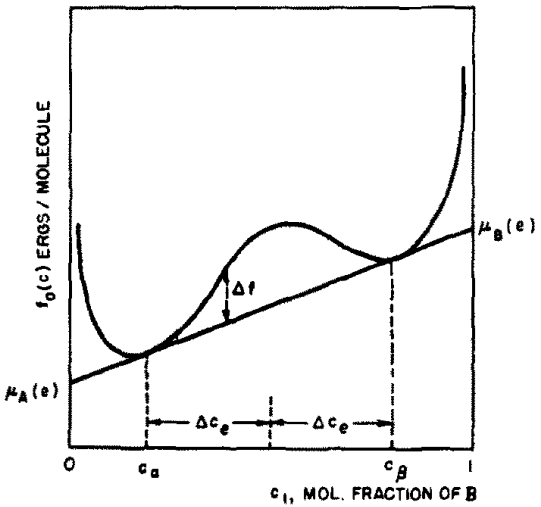

FIG. 1. $f_0(c)$ for $T<T_c$.

$$\gamma = 2N_V \int_{c_\alpha}^{c_\beta} \left(k\Delta f(c)\right)^{1/2} dc$$

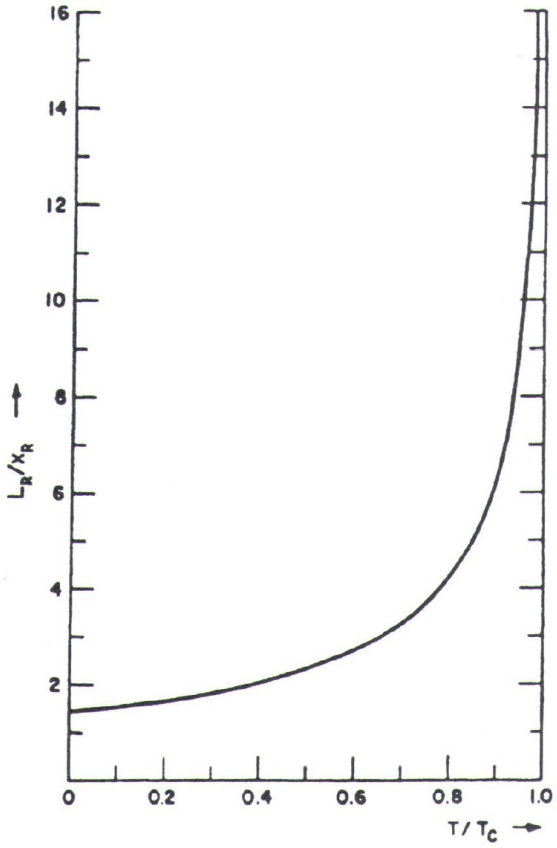

$$\gamma = 2N_V \int_{c_\alpha}^{c_\beta} \left(k\Delta f(c)\right)^{1/2} dc$$

$$\frac{dc}{dx} = \left(\frac{k}{\Delta f(c)}\right)^{1/2}$$

SuNMIL EPFL

Coherent Interfaces: The Cahn Hillard Model

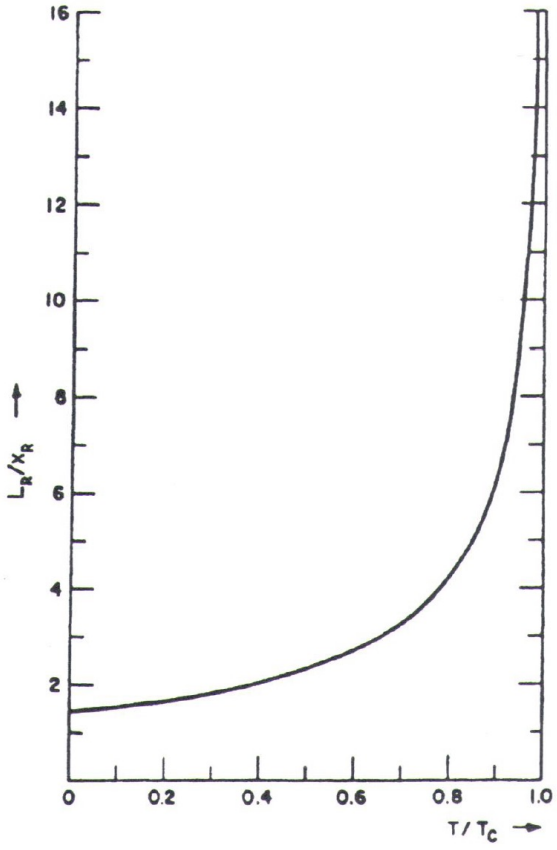

Thin Films in Modern Technology

- Growth of thin films of materials allows extreme control of the structure of matter at the nano-scale
- On the lab. scale: molecular beam epitaxy (MBE)
  - Extremely ''clean'' conditions, exquisite control of all parameters
  - Batch operation, extremely slow, ultra-high vacuum
- On the industrial level: chemical vapor deposition (CVD)
  - ''Dirtier'' operation, but much simpler to operate

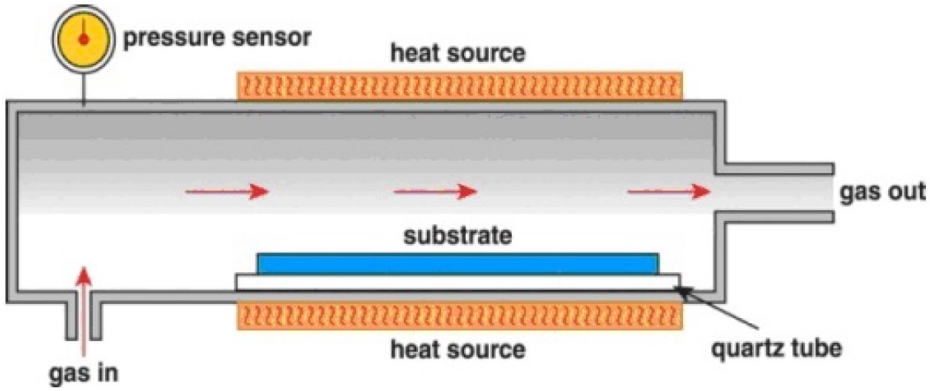

Thin Films – Morphology Control

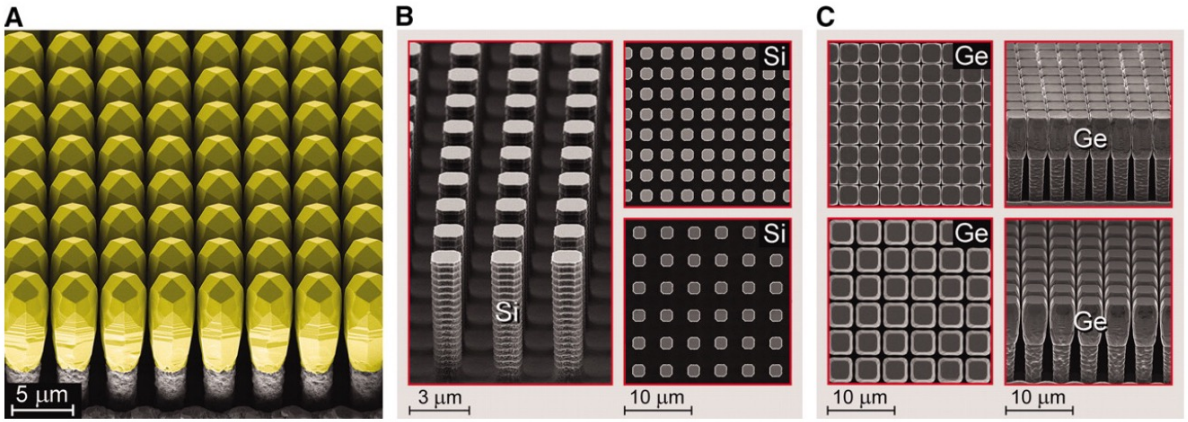

Strain-free Ge nanopillars grown by PECVD. [Falub et al., Science, 2012]

Growth Models for Thin Films

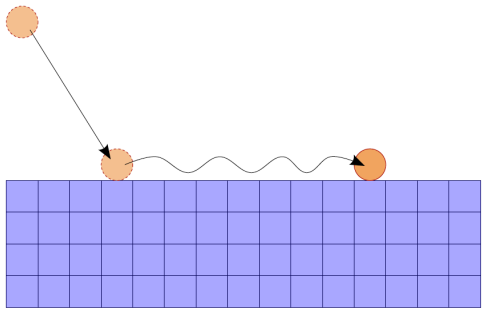

Growth Models for Thin Films

Frank-Van der Merwe

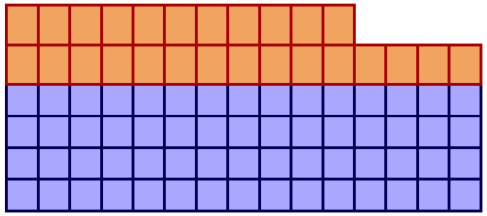

Volmer-Weber

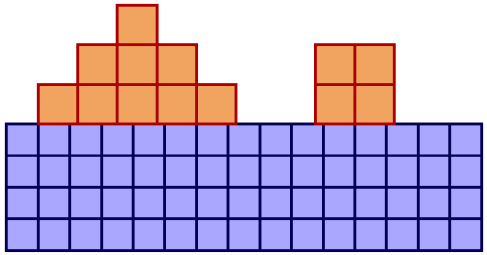

Stranski-Krastanov

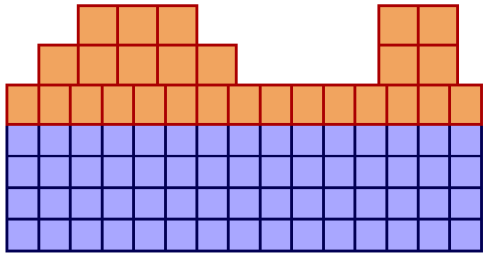

Growth Models for Thin Films

Frank-Van der Merwe

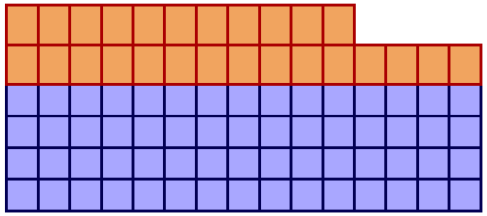

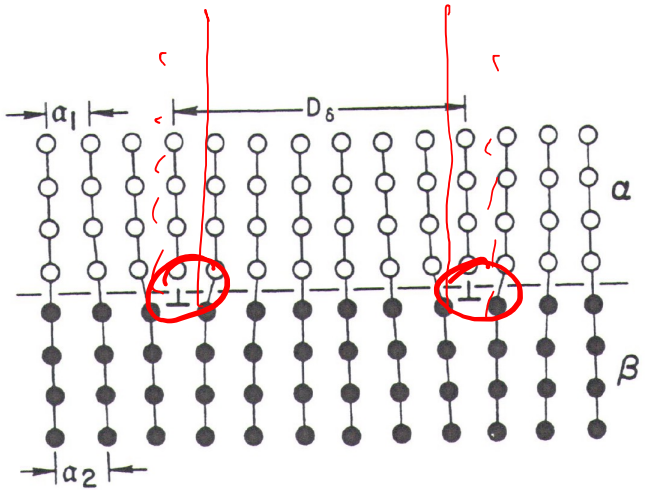

Growth Models for Thin Films: First Explanation

Frank-Van der Merwe

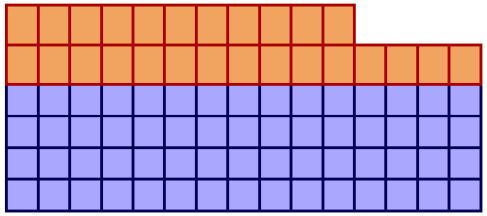

Volmer-Weber

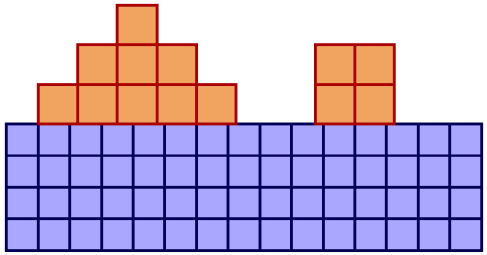

Stranski-Krastanov

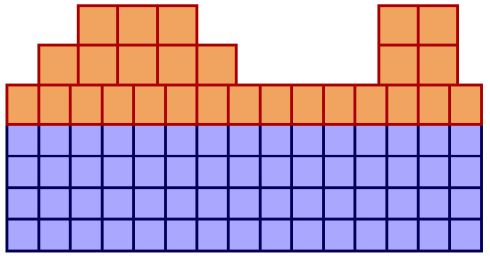

Growth Models for Thin Films: Second Explanation

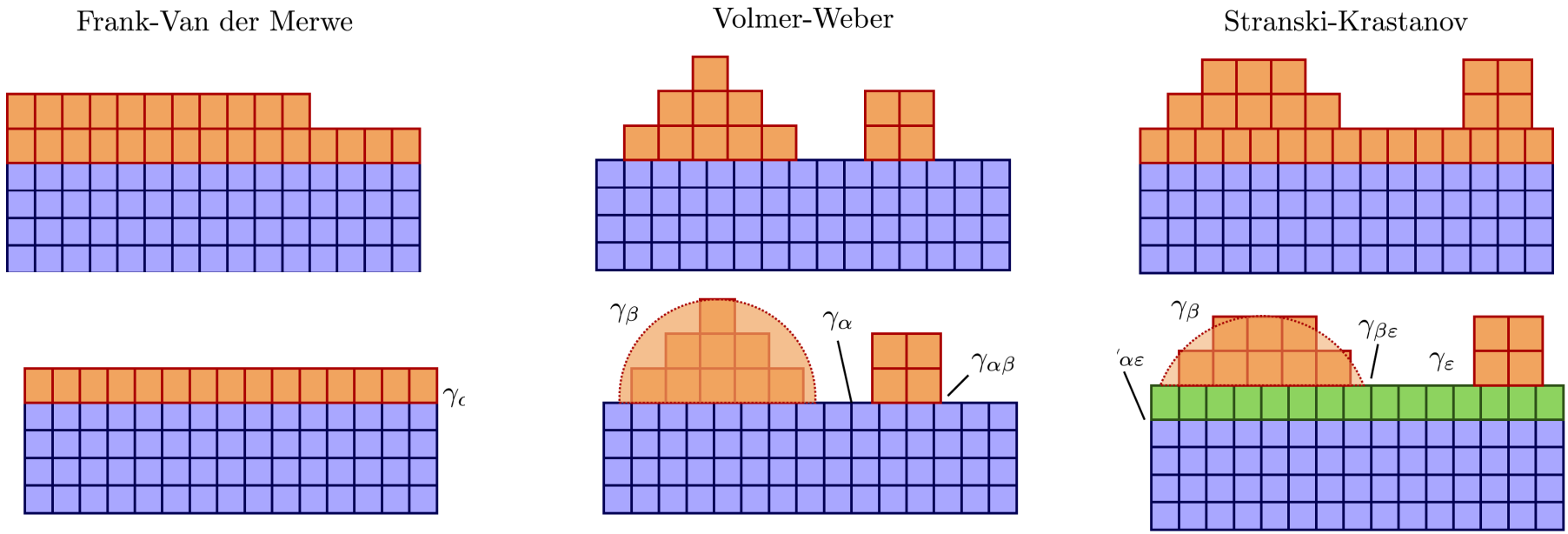

- Let's look at these from a macroscopic point of view: Recall Young's equation $\gamma_\beta \cos\theta = \gamma_\alpha - \gamma_{\alpha\beta}$
  - 3D Island (VW) growth corresponds to finite contact angle: $\gamma_{\alpha\beta} + \gamma_\beta > \gamma_\alpha$
  - Layer-by-layer (FM) growth corresponds to $\theta = 0$: $\gamma_{\alpha\beta} + \gamma_\beta \leq \gamma_\alpha$
  - Stranski-Krastanov growth is harder to explain based on macroscopic surface energies. If we consider the strained film as a different material ε, it must be that $\gamma_{\alpha\varepsilon} + \gamma_\varepsilon \leq \gamma_\alpha$, and $\gamma_{\beta\varepsilon} + \gamma_\beta > \gamma_\varepsilon$

Strained and Unstrained Growth

$$E_{el} = e^2 C_5 L_f$$

$$C_5 = 2\mu_f \frac{1+\nu_f}{1-\nu_f}$$

Growth Models for Thin Films: Third Explanation

Frank-Van der Merwe

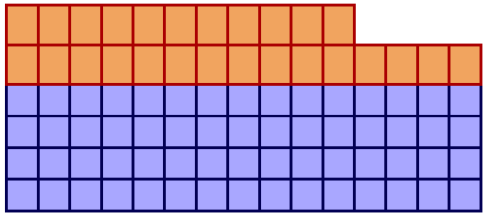

Volmer-Weber

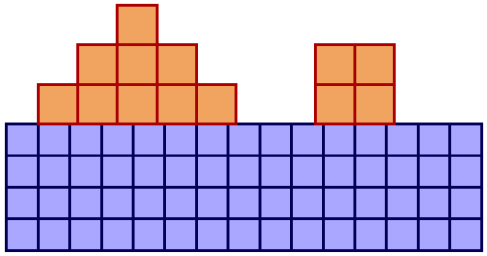

Stranski-Krastanov

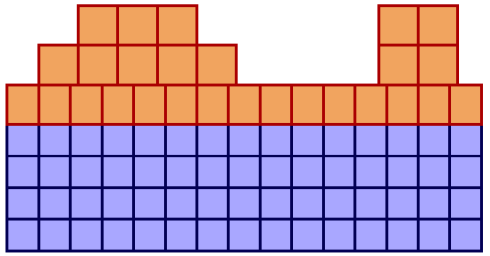

$$\mu(n) = \mu_\infty + [\varphi_a - \varphi'_a(n) + \varepsilon_d(n) + \varepsilon_e(n)]$$

$$\frac{d\mu}{dn} > 0$$

$$\frac{d\mu}{dn} < 0$$

Growth Models for Thin Films: Third Explanation

Frank-Van der Merwe

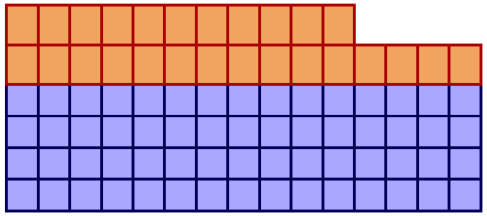

Volmer-Weber

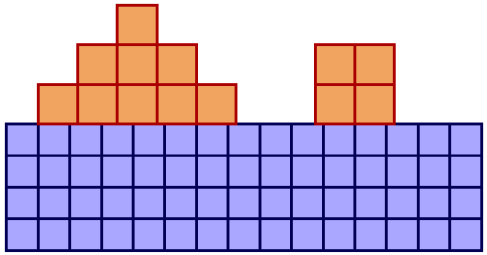

Stranski-Krastanov

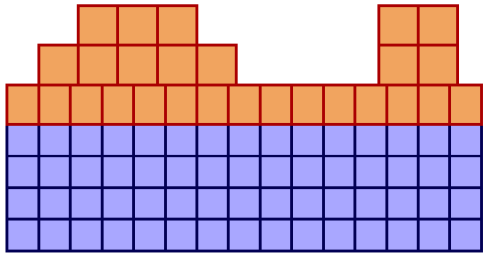

Growth Models for Thin Films

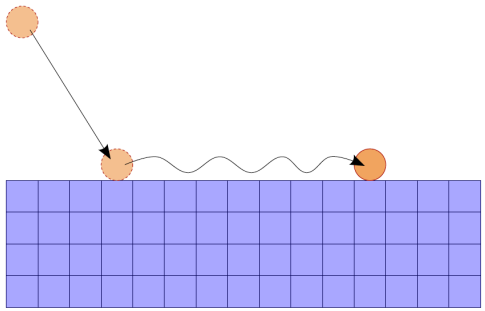

Diffusion Limited Aggregation

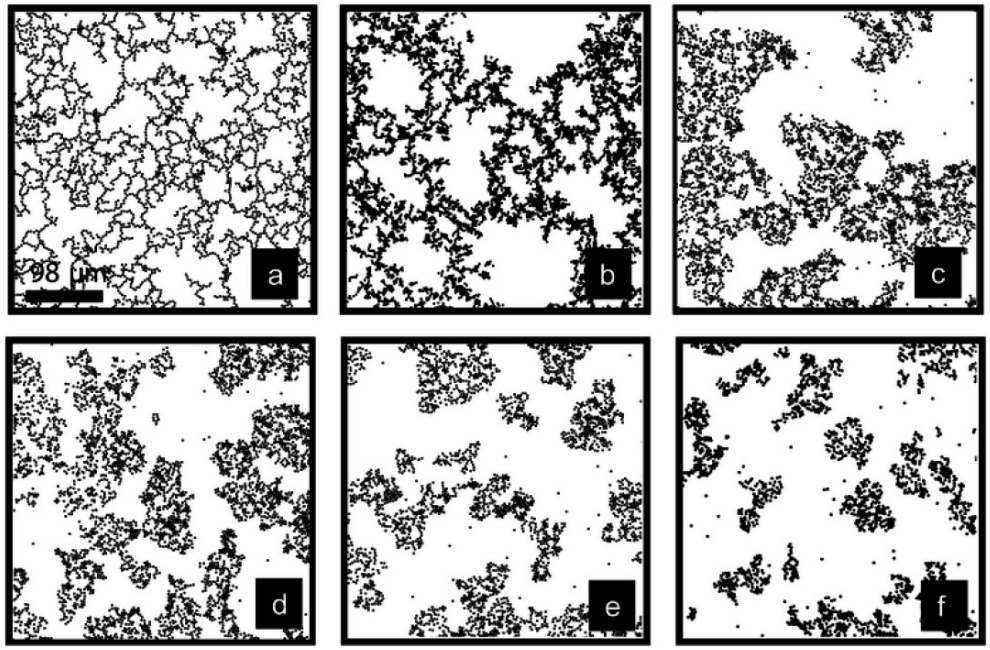

Flow-induced aggregation of colloids. [Massachaele et al., Soft Matter, 2011]

Diffusion Limited Aggregation

- Growth regimes discussed this far assume local equilibration between atom attachments
- The opposite case is a "stick where you hit" grow mode - strongly out of equilibrium structure
- Diffusion-limited aggregation

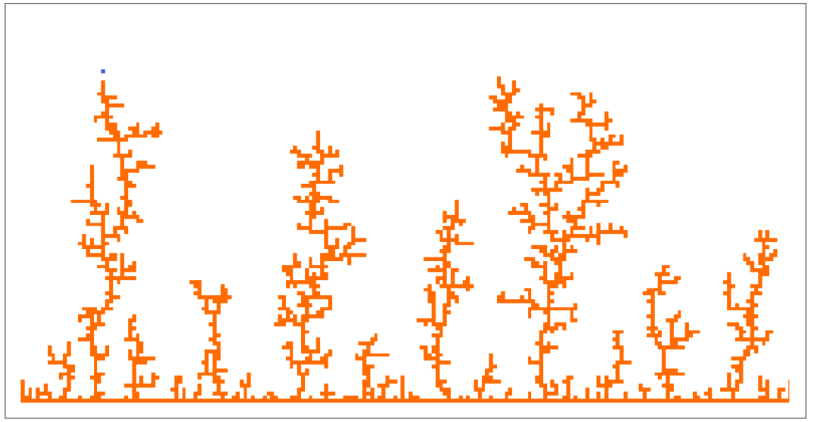

Conclusions

Conclusions